JOURNAL OF MOLECULAR SPECTROSCOPY **128**, 221–235 (1988)

The High-Resolution Fourier Transform Spectrum of Monoisotopic $C^{80}Se_2$ in the ν_2, ν_3, and $\nu_1 + \nu_3$ Regions: Equilibrium, Ground, and Excited State Parameters Determined by Rovibrational Analyses

HANS BÜRGER

Anorganische Chemie, FB 9, Universität, D-5600 Wuppertal 1, Federal Republic of Germany

AND

HELGE WILLNER

Institut für Anorganische Chemie, Universität, D-3000 Hannover,
Federal Republic of Germany

The IR spectrum of isotopically highly enriched (94.4% ^{80}Se) CSe_2 has been recorded with a resolution of 0.008 cm^{-1} in the ν_2 range near 310 cm^{-1} and 0.004 cm^{-1} in the ν_3 and $\nu_1 + \nu_3$ regions near 1300 and 1650 cm^{-1}, respectively. Data related to the lower states $n\nu_1$ and $m\nu_2^l$, $n + m \leqq 3$, have been obtained from an analysis involving 31 vibrational bands comprising a total of 4156 lines up to $J_{max} = 220$ which were fit with standard deviations ranging from 10 to 97 $\times 10^{-5}$ cm^{-1}. Band centers of $^{12}C^{80}Se_2$ were found at $\nu_1 = 369.1331(12)$, $\nu_2 = 313.0539(10)$, and $\nu_3 = 1301.8774(5)$ cm^{-1}. The rotational constants of the ground and equilibrium state were determined, $B_0 = 3677.325(8)$ and $B_e = 3683.344(18) \times 10^{-5}$ cm^{-1}, from which the bondlengths were derived, $r_0 = 1.6935536(19)$ and $r_e = 1.692169(3)$ Å. A local perturbation of the (30^01) state was observed, with (43^10) as supposed perturber acting by a $\Delta l = \pm 1$ mechanism. In addition, data are given for $^{13}C^{80}Se_2$, $^{12}C^{78}Se^{80}Se$, and $^{12}C^{80}Se^{82}Se$. © 1988 Academic Press, Inc.

I. INTRODUCTION

During the last decades infrared spectra in the region of the vibrational fundamentals ν_2 and ν_3 of the linear triatomics CO_2 (*1, 2*) and CS_2 (*3, 4*) have been repeatedly studied with high resolution. Combination, difference and hot bands as well as bands of isotopic varieties both with $D_{\infty h}$ and $C_{\infty v}$ symmetry have been thoroughly investigated. However, the heavier homolog CSe_2 has successfully resisted comparable efforts. Though CSe_2 was first synthesized in 1869 (*5*), the investigation of its molecular properties by spectroscopic methods has been effectively prevented by its instability at room temperature, the unpleasant odor even in high dilution, and the isotopic effect of selenium. The natural abundance of Se isotopes and their appropriate nuclear spin (0.87% ^{74}Se, $I = 0$; 9.02% ^{76}Se; $I = 0$; 7.58% ^{77}Se; $I = 1/2$; 23.52% ^{78}Se, $I = 0$; 49.82% ^{80}Se, $I = 0$; 9.19% ^{82}Se, $I = 0$) create a complex ensemble of CSe_2 isotopomers with $D_{\infty h}$ or $C_{\infty v}$ symmetry, which due to nuclear spin statistics populate J levels in a different fashion and hence their rovibrational spectra display different patterns. In view of this unfavorable situation, King and Srikameswaran, who studied the vibrational spectrum with prism infrared spectrometers (*6*) and the UV absorption spectrum

0022-2852/88 $3.00

(*7*), employed both natural material as well as samples highly enriched in ^{78}Se and ^{80}Se in order to overcome ambiguities caused by the isotopic effect.

Similarly, almost monoisotopic CSe_2 (95.45% ^{80}Se) was used by Maki and Sams (*8*) in the infrared investigation with a resolution of ca. 0.03 cm^{-1} of the combination bands $2\nu_1 + \nu_3$ and $2\nu_2^0 + \nu_3$ located at 2031 and 1922 cm^{-1}, respectively. The ground state rotational constant $B_0 = 0.0367831(100)$ cm^{-1} was determined from polynomial analyses of the rotational structure, and the equilibrium constant B_e and bondlength r_e were estimated.

Significantly better resolution of rovibrational spectra than that previously (*8*) available is demanded not only by the smallness of the rotational constant but also by the overlap with hot bands, keeping in mind that at 298 K the population of the $v_1 = 1$ and $v_2 = 1$ vibrational states, $\nu_1^0 \simeq 369$ and $\nu_2^0 \simeq 313$ cm^{-1}, relative to the ground state is 17 and 44%, respectively. In order to determine accurately the equilibrium, ground, and vibrationally excited state parameters of one pilot isotopic species of CSe_2, to map its rovibrational energy levels, to determine anharmonic constants, and to search for perturbations, we have initiated a high-resolution study of highly enriched $C^{80}Se_2$ in the region of the three most intense absorptions, which are in the order of decreasing intensity ν_3 near 1300 cm^{-1}, ν_2 near 313 cm^{-1}, and $(\nu_1 + \nu_3)$ near 1665 cm^{-1}. The available resolution (FWHM) in the ν_3 and $(\nu_1 + \nu_3)$ regions was $\sim 4 \times 10^{-3}$ cm^{-1}, while the ν_2 band was studied with a resolution of $\sim 8 \times 10^{-3}$ cm^{-1}. In the present contribution we report on our results obtained for $^{12}C^{80}Se_2$ but also give data for the isotopic varieties $^{13}C^{80}Se_2$, $^{12}C^{78}Se^{80}Se$, and $^{12}C^{80}Se^{82}Se$ which were present as minor constituents in our sample.

II. EXPERIMENTAL DETAILS

Isotopically enriched CSe_2 was prepared in analogy to Ref. (*7*) from elemental Se (Oak Ridge, 94.4% ^{80}Se, 2.4% ^{82}Se, 2.0% ^{78}Se, 0.6% ^{77}Se, 0.5% ^{76}Se) and natural CH_2Cl_2 according to the equation

$$CH_2Cl_2 + 2Se \rightarrow CSe_2 + 2HCl.$$

For this purpose, 100 mg (1.25 mmole) Se was placed in a 30-ml Pyrex ampoule, which measured 20 × 140 mm and was connected to a 6-mm-o.d. tube 200 mm long. After evacuation 2 mmole dry CH_2Cl_2 was condensed onto the selenium, and the ampoule was sealed and heated to 570°C for 1 hr. Unreacted Se, deposited at the end of the 6-mm tube, was sublimed by heating into the ampoule held at −196°C. Then the tube was connected to a vacuum line employing a recently described device (*9*) and opened and the major quantity of HCl and CH_2Cl_2 was pumped off at −80°C. Thereafter the residue was purified *in vacuo* by fractional condensation in traps held at −20, −90, and −196°C. CSe_2 was collected in the −90°C trap. In order to enhance the yield the unreacted residual Se was then treated repeatedly in the same fashion with 2 mmole CH_2Cl_2. The yield of CSe_2 was ca. 15% for each of the first three reaction cycles. CSe_2 was stored in the dark at −198°C.

Infrared spectra were recorded with a prototype version of the Bruker IFS 120 HR vacuum spectrometer (*10*). The ν_2 band near 310 cm^{-1} was measured with an apodized resolution of 0.0078 cm^{-1} employing a globar source, a 3.5-μm Mylar beamsplitter, and a liquid He-cooled Si bolometer. Due to energy cutoff, a *S:N* ratio of only 25 was achieved by coadding 64 scans. The coaddition of scans was limited by the fact that sample was lost by obvious diffusion through the polythene windows when the (otherwise tight) cell was exposed to the vacuum of the interferometer. A glass cell measuring 18.7 cm was employed, and a pressure of (initially) 9 mbar was chosen. Calibration was with H_2O rotational lines (*11*), and the absolute wavenumber accuracy of stronger peakfinder evaluated lines was $\pm 1 \times 10^{-3}$ cm^{-1}. Positions of some weak absorptions were estimated visually.

The ν_3 and $\nu_1 + \nu_3$ bands near 1300 and 1660 cm^{-1}, respectively, were measured with an apodized resolution of 0.0039 cm^{-1} employing a globar source, KBr beamsplitter, and a liquid N_2-cooled MCT detector. An optical broadband filter was used to eliminate radiation >1900 and <1000 cm^{-1}. A glass cell measuring 20 cm with KBr windows was employed, and pressures of 2 and 0.3 mbar were chosen. One hundred twenty and 150 scans were coadded respectively, and a *S:N* ratio $\geqslant 100$ was achieved. With a Doppler width at 298 K and 1300 cm^{-1} of 0.0013 cm^{-1}, the actual linewidth (FWHM) was ca. 0.004 cm^{-1}.

Calibration was carried out by comparison with lines of the ν_2 band of N_2O (*11*), which were fitted with a rms deviation of 6×10^{-5} cm^{-1}. The calibration in the 6-μm region was furthermore checked with H_2O lines (*11*). The assumed absolute and relative wavenumber accuracy of unblended lines are 5×10^{-4} and 1×10^{-4} cm^{-1} for the ν_3 band and 1×10^{-3} and 2×10^{-4} cm^{-1} for the (weaker) $\nu_1 + \nu_3$ band as well as the ν_3 band of $^{13}C^{80}Se_2$.

III. DESCRIPTION OF THE SPECTRA

The spectra of CSe_2 in the region of the fundamental ν_2 and of the vibrations ν_3 and $\nu_1 + \nu_3$ have the typical appearance of Σ–Π and Σ–Σ bands, respectively, of a linear molecule and are similar to those of the thoroughly investigated lighter homologs CO_2 and CS_2. Despite the population of higher *J* levels, the bands are narrower due to the much smaller *B* value, 3.7×10^{-2} cm^{-1} (cf. CO_2 39.0 and CS_2 10.9×10^{-2} cm^{-1}). The density of the rotational structure is further enhanced by the greater importance of hot bands. On the other hand, there is no overlap of the ν_3 bands of $^{12}CSe_2$ and $^{13}CSe_2$ due to the large isotopic shift, $\Delta\nu_3 = 47.0$ cm^{-1}, which may be compared with that of CO_2, 65.7 cm^{-1}, and CS_2, 50.0 cm^{-1}.

(a) The ν_2 Band

The ν_2 band near 310 cm^{-1} reveals a prominent, blue-degraded *Q* branch at 313.054 cm^{-1} which was resolved into *J* lines for $J'' \geqslant 20$ and which could be followed over 1.8 cm^{-1} up to $J'' = 146$. The 4*B* spacing of the *P*- and *R*-branch lines, which were also followed up to $J'' = 146$, decreases to smaller wavenumbers, which is in agreement with the expected negative α_2^B value.

The cold band ν_2 is accompanied by three hot bands with band centers at 310.128, 317.711, and 313.542 cm^{-1}. The *Q* branches of the two former bands reveal a line pattern similar to that of ν_2 as well as 4*B*-spaced *R*- and *P*-branch lines and are thus assigned to one of the Σ_g^+–Π_u transitions (11^10–10^00) and (02^00–01^10). In contrast, the *Q* branch of the latter band was not resolved, at least for the more intense small

J values, and furthermore buried under the dominating Q branch of the cold band. In agreement with its assignment to the $(02^20\text{–}01^10)$ band, the c and d lines in the P and R branches with J'' odd and even reveal alternating spacings indicating a $(q'\text{-}q'')$ value different from zero. Though the hot bands $(11^10\text{–}10^00)$ and $(02^00\text{–}01^10)$ can hardly be distinguished by their intensities, their assignment follows unambiguously from their B'' values determined in the rotational analyses and independently from the combination difference $(02^00\text{–}01^10) = (02^01\text{–}00^00) - (02^01\text{–}02^00) - (01^10\text{–}00^00)$, $\nu^{BC}_{\text{calc}} = 317.705\ \text{cm}^{-1}$, employing a value $(02^01\text{–}00^00) = 1922.0135\ \text{cm}^{-1}$ determined for $^{12}C^{80}Se_2$ by Maki and Sams (*8*).

No further bands due to hot bands or isotopic varieties could be assigned with certainty.

(b) *The ν_3 and $\nu_1 + \nu_3$ Bands*

The appearance of the ν_3 and $\nu_1 + \nu_3$ bands is very similar. Their most pronounced features are the R-branch heads of the cold bands near 1307.5 and 1671.7 cm^{-1}, respectively, at the high wavenumber end of the bands. The bandhead of the ν_3 band is illustrated in Fig. 1, and evidently the R-branch lines can be followed beyond the turnover to lower wavenumbers up to $R(204)$. Lines originating from $^{12}C^{78}Se^{80}Se$ are also assigned in Fig. 1, and some additional, unmarked features due to $^{12}C^{77}Se^{80}Se$ and $^{12}C^{76}Se^{80}Se$ are present as well. A similar bandhead has also been observed in the $(10^01\text{–}00^00)$ band of CS_2 (see Fig. 1 in Ref. (*12*)). The approximate J'' values at the turnovers of ν_3 and $\nu_1 + \nu_3$ are 148 and 130, respectively. The J'' assignments were unambiguously determined by the $6B$ gap in the band centers. This is illustrated for the $\nu_1 + \nu_3$ system in Fig. 2, in which also the bandhead of the first hot band associated with the transition $(20^01\text{–}10^00)$ is visible.

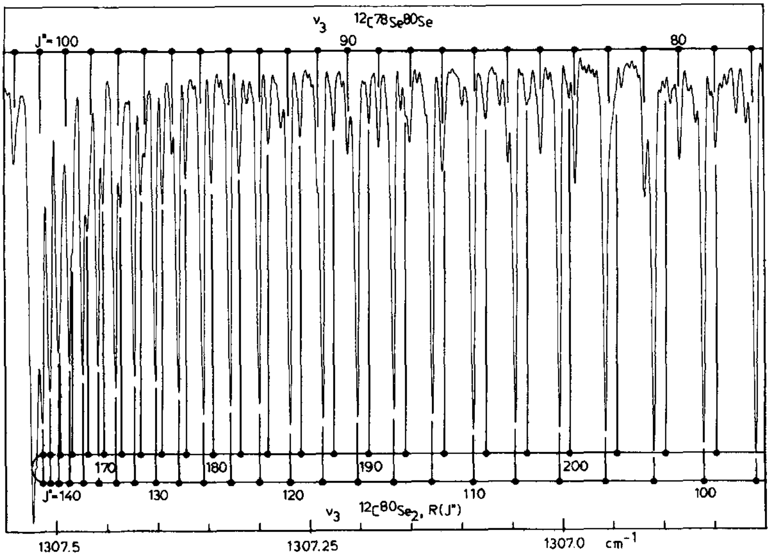

FIG. 1. Detail of the ν_3 band of CSe_2 showing the R-branch head of $^{12}C^{80}Se_2$ and a portion of the R branch of $^{12}C^{78}Se^{80}Se$, with J'' assignments indicated; 20-cm cell, 0.3 mbar.

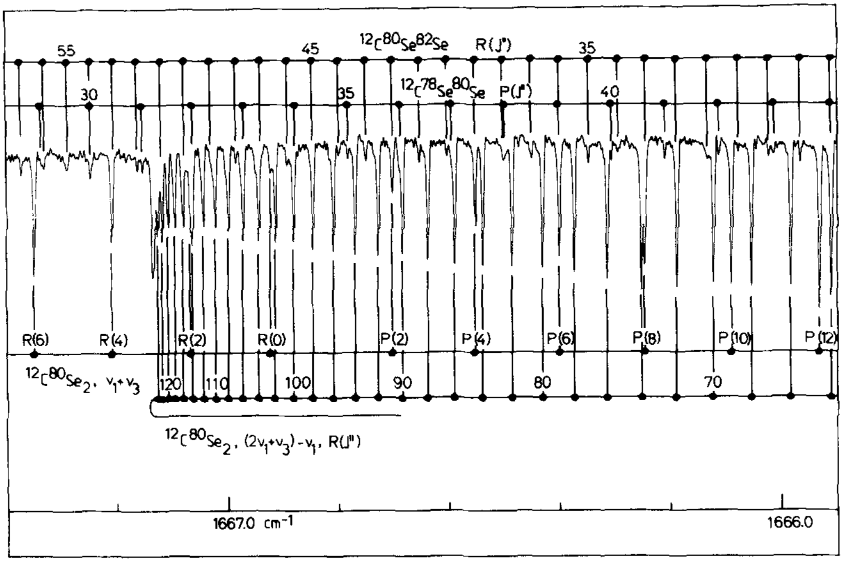

FIG. 2. Detail of the $\nu_1 + \nu_3$ band of CSe_2 with band center of $C^{80}Se_2$, portions of the *R* branch of $^{12}C^{80}Se^{82}Se$ and *P* branch of $^{12}C^{78}Se^{80}Se$, and *R*-branch head of the hot band (20^01–10^00) of $^{12}C^{80}Se_2$. *J"* assignments are given; 20-cm cell, 2 mbar.

To the lower wavenumbers the rotational structure expands more and more until for the highest *J* values discernible in the *P* branches the separation of successive lines of ν_3 and $\nu_1 + \nu_3$ of $C^{80}Se_2$ is on the order of $10B$.

Despite this increasing spread of lines when proceeding to lower wavenumbers, the complexity of the spectra grows because more and more hot bands become important. These are displaced from the cold bands $\nu_1/(\nu_1 + \nu_3)$ regularly and uniformly to lower wavenumbers by $\sim v_1 \times 4.2/4.5$ cm^{-1} and $\sim v_2 \times 5.3/8.3$ cm^{-1}, respectively. The same displacements are also retained in hot bands with lower states excited in both v_1 and v_2. Though the *J* assignment of the weaker hot bands may not be evident from features associated with the band center, it follows unambiguously from the observation of several bands with common (upper or lower) states, the large α^B values, the substantial *q* values for Π states, and the number of (nearly) equidistant and equally intense lines associated with transitions involving degenerate states. A portion of the congested *P*-branch region is shown in Fig. 3. Hot bands ($nv_1mv_2^l1 - nv_1mv_2^l0$) of ν_3 have been systematically assigned up to $n + m = 3$, and all vibrational energy levels of $^{12}C^{80}Se_2$ up to ~ 1000 cm^{-1} above the ground state can thus be determined. While the hot bands with $3\nu_2$ as lower state were assigned quite easily due to their large shifts from ν_1 (~ -16 cm^{-1}) and their prominence in the expanded *P* branch, the hot band (30^01–30^00) was much less pronounced despite its only slightly smaller Boltzmann factor because, due to its smaller displacement from ν_1, ~ -12 cm^{-1}, it occurs in a more congested spectral region.

This experience is an important aid for estimating the chance of finding the $2\nu_3 - \nu_3$ hot band, without which the complete set of harmonic vibrational frequencies cannot be determined at present. If we assume that the anharmonicity constant x_{33}

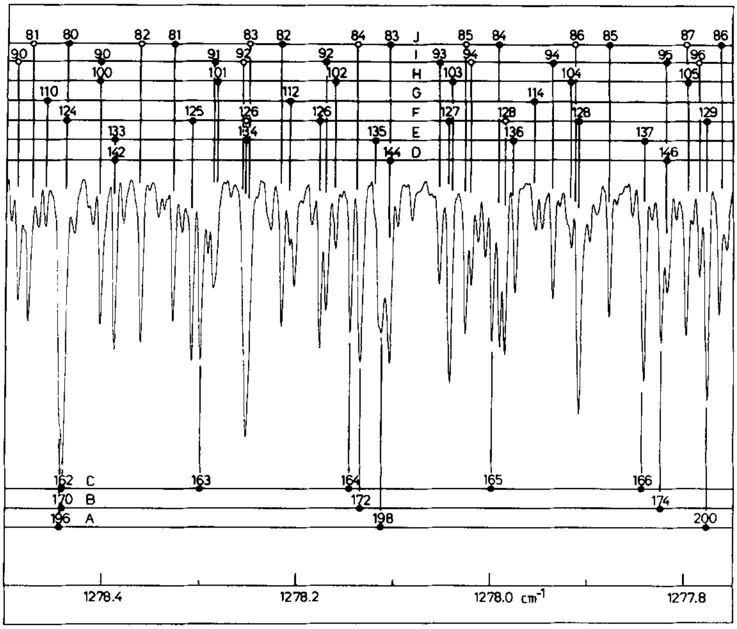

FIG. 3. Detail of the P branch of ν_3 of $^{12}C^{80}Se_2$. J'' assignments are given for the following vibrational transitions: A, (00^01–00^00); B, (10^01–10^00); C, (01^11–01^10); D, (20^01–20^00); E, (11^11–11^10); F, solid dots (02^21–02^20), open dots (02^01–02^00); G, (30^01–30^00); H, (21^11–21^10); I, solid dots (12^21–12^20), open dots (12^01–12^00); J, solid dots (03^31–03^30), open dots (03^11–03^10); 20-cm cell, 2 mbar.

is smaller in CSe_2 than in CS_2, ~ -6.5 cm^{-1} (*13*), a search for this hot band in the spectra available to us appears hopeless. The vibrational bands of $^{12}C^{80}Se_2$ assigned in the present study are indicated by vertical arrows in the energy level diagram (Fig. 4).

The ν_3 and $\nu_1 + \nu_3$ bands of $^{12}C^{78}Se^{80}Se$ and $^{12}C^{80}Se^{82}Se$ have been observed and assigned as well, and due to their large isotopic displacements the bands (00^01–00^00), (10^01–10^00), and (01^11–01^10) of $^{13}C^{80}Se_2$ have also been measured.

IV. THEORY AND DATA REFINEMENT

The present study follows the conventional formalism adopted in previous investigations of CO_2 (*1*) and CS_2 (*3, 4*). With a term value given by

$$T_v = G_v + B_v[J(J+1) - l^2] \pm 1/2q_vJ(J+1) - D_v[J(J+1) - l^2]^2 \qquad (1)$$

the vibrational term difference ν_0 is defined by

$$\nu_0 = G_v' - G_v'' \qquad (2)$$

and connected to the effective band center ν_{BC} by

$$\nu_{BC} = \nu_0 - (B'l'^2 - B''l''^2 \pm 1/2(q'l'^2 - q''l''^2)). \qquad (3)$$

Higher order terms of Eq. (1), e.g., H_v and μ_v (the $J(J+1)$ dependence of q_v), were omitted because in the analysis of the bands most favorable for their determination,

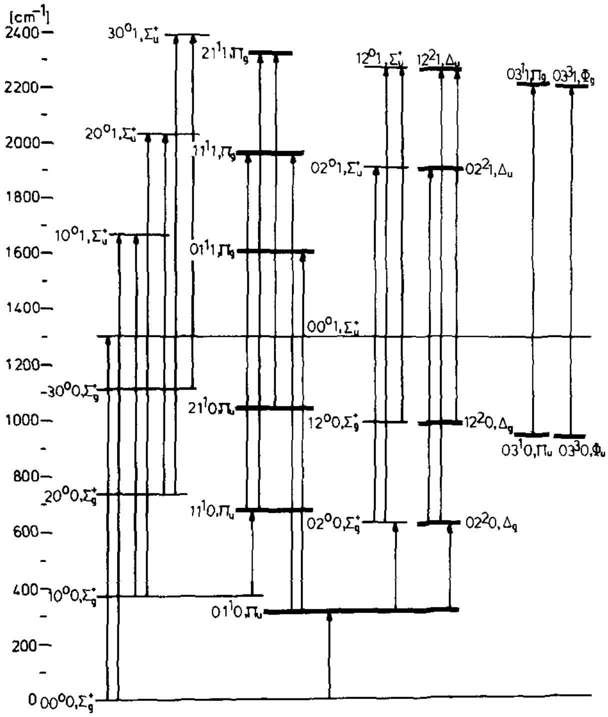

FIG. 4. Vibrational energy level diagram of $^{12}C^{80}Se_2$. Arrows indicate transitions investigated in the present study.

(00^01–00^00) and (01^11–01^10), respectively, their values did not exceed three of their standard deviations, and their inclusion did not improve the respective fits.

The Σ–Σ transitions were fit to the polynomial

$$\nu_{P,R} = a + bm + cm^2 + dm^3 + em^4 \tag{4}$$

by least-squares methods with the approximations

$$a = \nu_{\mathrm{BC}}$$

$$b = (B' + B'')$$

$$c = (B' - B'')$$

$$d = -2(D' + D'')$$

$$e = -(D' - D'')$$

and $m = -J''$ and $(J'' + 1)$ in the P and R branch, respectively.

Though transitions of ν_3 and $\nu_1 + \nu_3$ were measured simultaneously and with comparable accuracy, nevertheless weak features were, due to the higher intensity, more significant in the ν_3 band. Therefore the lower states of the $(\nu_1 + \nu_3)$ band of $^{12}C^{78}Se^{80}Se$ and $^{12}C^{80}Se^{82}Se$ were constrained to the ground states as determined by the analysis of the appropriate ν_3 band. On the other hand, the (21^11) and (12^01) states reached by the hot bands (21^11-21^10) and (12^01-12^00) were constrained to the parameters following from the (more significantly determined) (21^11-11^10) and (12^01-02^00) hot bands, keeping in mind that errors associated with such constraints of correlated parameters are frequently underestimated. Statistical data and the results of the polynomial analyses in terms of rovibrational parameters are set out in Tables I and II.

For transitions involving degenerate (Π, Δ, Φ) states a different procedure was adopted in order to make use of justified constraints as far as possible and to circumvent the correlations of lower and upper state parameters whenever possible. The method chosen uses combination differences between transitions reaching a common upper

TABLE I

Statistics for the CSe_2 Bands Measured

Species Transition	J''_{max} in P branch	J''_{max} in R branch	No. of nonzero weighted lines	Standard deviation σ ($10^{-5}cm^{-1}$)
$^{12}C^{80}Se_2$				
01^10-00^00	146	126 (142)^a	158	69
11^10-10^00	106	104 (108)^a	92	88
02^00-01^10	81	99 (108)^a	74	69
02^20-01^10	100	109	135	97
00^01-00^00	220	204	170	10
10^01-10^00	204	186	131	12
20^01-20^00	178	132	88	30
30^01-30^00	128	100	39	33
01^11-01^10	204	141	263	12
11^11-11^10	183	138	207	19
21^11-21^10	153	111	123	34
02^01-02^00	186	126	114	26
12^01-12^00	158	114	68	32
02^21-02^20	199	131	229	20
12^21-12^20	178	122	160	35
03^11-03^10	162	114	172	29
03^31-03^30	178	115	192	30
10^01-00^00	196	186	149	11
20^01-10^00	166	122	110	17
30^01-20^00	126	124	79	26
11^11-01^10	159	125	213	16
21^11-11^10	139	130	187	29
12^01-02^00	130	124	75	32
12^21-02^20	135	116	153	34
$^{13}C^{80}Se_2$				
00^01-00^00	174	152	150	11
10^01-10^00	152	140	97	18
01^11-01^10	148	144	234	14
$^{12}C^{78}Se^{80}Se$				
00^01-00^00	138	143	160	22
10^01-00^00	94	108	115	45
$^{12}C^{80}Se^{82}Se$				
00^01-00^00	153	134	154	19
10^01-00^00	-	108	57	50

$^a J''_{max}$ in Q branch.

state, e.g., $P(J'' + 1)$ and $R(J'' - 1)$ lines, to determine the lower state parameters. Since these are independent of the excited states reached by the respective transitions, in principle all available pairs of lines, e.g., with (01^10) as the lower state, in detail those from the $(01^11\text{-}01^10)$, $(11^11\text{-}01^10)$, $(02^20\text{-}01^10)$, and $(02^00\text{-}01^10)$ bands, may be treated in one common analysis to yield the parameters B^c_2, B^d_2, D^c_2, and D^d_2 of the (01^10) state.

We have found that the difference $D^c_v - D^d_v$ could never be determined significantly, and therefore it was constrained to zero. In fact B'', D'', and q'' were the parameters which were independently refined by a least-squares procedure. For the Δ and Φ states, q_v did not differ significantly from zero and therefore was neglected.

Only unit-weighted lines belonging to the ν_3 and $\nu_1 + \nu_3$ bands were used to form pairs of lower state combination differences, lines of the ν_2 band being rejected because of their poorer quality. The results of the respective analyses are set out in Table III. These lower state parameters were used as constraints in the fit of transitions and are bracketed in Table II.

TABLE II

Results of Rovibrational Analyses

Species	ν_{BC}	B''	B'	$B''-B'$	D''_J	D'_J	$D''_J-D'_J$	q''	q'	$q''-q'$
Transition	(cm^{-1})		(10^{-5}cm^{-1})			(10^{-10}cm^{-1})			(10^{-5}cm^{-1})	
$^{12}C^{80}Se_2$										
01^10-00^00	313.053 86(12)[a]	[3677.325][b]	3685.195	-7.870(3)	[14.49]	14.736	-0.246(18)		1.0743(13)	
11^10-10^00	310.128 14(30)	[3673.25]	3681.55	-8.301(12)	[14.49]	14.98	-0.49(10)		1.117(3)	
02^00-01^10	317.710 61(19)	[3685.194]	3692.374	-7.180(3)	[14.76]	14.76	0.0	[1.074]	0.0	1.074
02^20-01^10	313.541 51(23)	[3685.194]	3693.084	-7.890(11)	[14.76]	15.46	-0.70(10)	[1.074]	0.0220	1.0520(31)
00^01-00^00	1301.877 391(15)	3677.325(8)	3653.616	23.708 4(2)	14.494(16)	14.518	-0.023 8(6)			
10^01-10^00	1297.714 135(23)	3673.256(12)	3649.536	23.720 2(4)	14.477(26)	14.494	-0.017 3(10)			
20^01-20^00	1293.540 54(8)	3669.26(6)	3645.54	23.719 7(18)	14.53(25)	14.58	-0.048(9)			
01^11-01^10	1296.522 428(16)	[3685.194]	3661.570	23.622 9(3)	[14.76]	14.78	-0.028 0(5)	[1.074]	1.069	0.005 38(14)
11^11-11^10	1292.309 56(3)	[3681.554]	3657.938	23.616 2(7)	[14.64]	14.66	-0.022 0(23)	[1.117]	1.115 7	0.001 3(3)
21^11-21^10	1288.088 17(5)	3677.95	[3654.355]	23.614 9(5)	14.73	[14.73]	0.0	1.158	[1.158]	0.00
02^01-02^00	1291.254 46(4)	3692.37(4)	3668.80	23.563 2(9)	14.58(20)	14.62	-0.038(5)			
12^01-12^00	1287.006 92(6)	3689.02	[3665.47]	23.552 1(9)	14.6	[14.6]	0.0			
02^21-02^20	1291.175 66(3)	[3693.006]	3669.467	23.537 9(6)	[15.01]	15.03	-0.024 5(18)	0.0	0.003 23	-0.003 23(26)
12^21-12^20	1286.920 92(6)	[3689.990]	3666.477	23.513 3(12)	[15.95]	16.00	-0.045(4)			
03^11-03^10	1285.985 03(5)	[3699.62]	3676.12	23.500 2(11)	[14.73]	14.75	-0.020(4)	[2.06]	2.047	0.012 5(4)
03^31-03^30	1285.836 90(4)	[3700.90]	3677.45	23.452 2(9)	[15.7]	15.73	-0.034			
10^01-00^00	1666.847 225(17)	3677.372(11)	3649.619	27.752 4(3)	14.632(26)	14.709	-0.076 9(11)			
20^01-10^00	1662.323 84(4)	3673.296(28)	3645.549	27.747 5(11)	14.34(13)	14.43	-0.087(6)			
11^11-01^10	1658.516 600(19)	[3685.194]	3657.954	27.240 0(5)	[14.76]	14.90	-0.135 7(2)	[1.074]	1.108	-0.034 14(23)
21^11-11^10	1654.308 91(4)	[3681.554]	3654.334	27.219 6(12)	[14.64]	14.73	-0.089(7)	[1.117]	1.158	-0.0413(5)
12^01-02^00	1650.040 23(10)	3692.34(8)	3665.47	26.875(3)	14.7(4)	14.9	-0.117(22)			
12^21-02^20	1650.359 06(5)	[3693.006]	3666.225	26.780 6(18)	[15.01]	15.17	-0.157(13)			
$^{13}C^{80}Se_2$										
00^01-00^00	1254.903 490(18)	3677.448(13)	3654.653	22.795 2(4)	14.46(4)	14.48	-0.023 6(18)			
10^01-10^00	1250.886 62(4)	3673.407(28)	3650.603	22.803 8(12)	14.43(10)	14.46	-0.020(6)			
01^11-01^10	1249.943 277(19)	[3685.010]	3662.296	22.711 0(5)	[14.64]	14.67	-0.030 9(28)	[1.125]	1.119	0.005 96(19)
$^{12}C^{78}Se^{80}Se$										
00^01-00^00	1302.444 55(4)	3724.45(3)	3700.44	24.017 6(12)	14.89(13)	14.89	-0.007(7)			
10^01-00^00	1669.721 64(12)	[3724.45]	3696.33	28.125(5)	[14.89]	15.04	-0.16(5)			
$^{12}C^{80}Se^{82}Se$										
00^01-00^00	1301.338 87(4)	3632.383(26)	3608.963	23.420 1(11)	13.90(12)	13.91	-0.007(6)			
10^01-00^00	1664.094 08(23)	[3632.383]	3604.999	27.384(9)	[13.90]	14.07	-0.16(7)			

[a] One standard deviation in parentheses. See text for possible calibration error. [b] Constrained parameters in brackets.

TABLE III

Fits of Lower States by Combination Differences for CSe_2

Lower State	Upper States	B" $10^{-5}cm^{-1}$	D" $10^{-10}cm^{-1}$	q" $10^{-5}cm^{-1}$	No. of differences	σ $10^{-5}cm^{-1}$
$^{12}C^{80}Se_2$						
20^00	20^01, 30^01	3669.26(5)	14.61(22)	0.0	34	38
01^10	01^11, 11^11	3685.194(11)	14.76(4)	1.055(8)	142	16
11^10	11^11, 21^11	3681.554(28)	14.64(12)	1.117(20)	87	28
02^20	02^21, 12^21	3693.006(27)	15.01(14)	0.0	72	31
03^10	03^11	3699.62(10)	14.7(7)	2.06(9)	18	43
03^30	03^31	3700.90(6)	15.7(3)	0.0	16	30
12^20	12^21	3689.99(6)	15.95(26)	0.0	14	28
$^{13}C^{80}Se_2$						
01^10	01^11	3685.010(13)	14.64(5)	1.125(10)	85	14

For the (21^11-21^10) hot band, too few unit-weighted R-branch lines corresponding to unit-weighted P-branch lines were available to determine with significance the parameters of the (21^10) state. Therefore, the upper state was constrained to the parameters obtained from the (21^11-11^10) band, and the lower state parameters were refined. The values determined by combination differences agree with these to within three of their standard deviations.

Since the above-mentioned method, which takes advantage of the high relative accuracy of the FT spectra, is similarly applicable to Σ states, it is also amenable to the perturbed (30^01-20^00) transition (see below), the lower state of which was determined jointly with that of the (20^01-20^00) band (Table III). Finally, the ground and $v_1 = 1$ state parameters determined from the 1300 cm^{-1} band were employed in the analysis of the (01^10-00^00) and (11^10-10^00) transitions.

A total of 4156 nonzero-weighted lines belonging to 31 vibrational bands were subjected to least-squares fits to yield the parameters listed in Table II. Details concerning the data composition and standard deviation of the fits are quoted in Table I. Due to blending, about 25% of the lines, in particular those of hot bands, were therefore given a lower weight (0.1), as well as those of the 310 cm^{-1} bands which were visually measured. The fits converged with standard deviations ranging from 10 to 97×10^{-5} cm^{-1} which correspond to 1/40 to 1/10 of the resolution of the spectra. Clearly the fits were better for the stronger bands than for the weaker ones. Lists of observed and calculated transition wavenumbers have been deposited as supplementary material.[1]

---

[1] Lists of observed and calculated transition wavenumbers (87 pp.) have been deposited in the Editorial Office of the *Journal of Molecular Spectroscopy* and may be obtained from Fachinformationszentrum Energie–Physik–Mathematik, D-7514 Eggenstein, Leopoldshafen, West Germany, on submission of the names of the authors, the literature reference, and the registry number IRD-10029.

The transitions (30^01–20^00) and (30^01–30^00) turned out to be perturbed due to a rotational resonance affecting the (30^01) state. Their analysis is reported in the next section.

Some molecular parameters of CSe_2 derived from the data of Tables II and III are collected in Table IV. The α^B and β values refer to the respective $v = 1 \leftarrow 0$ transitions. The equilibrium rotational constant B_e and the centrifugal distortion constant D_e of $^{12}C^{80}Se_2$ and $^{13}C^{80}Se_2$ were calculated according to

$$B_e = B_0 + 1/2\alpha_1^B + \alpha_2^B + 1/2\alpha_3^B \tag{5}$$

and

$$D_e = D_0 - 1/2\beta_1 - \beta_2 - 1/2\beta_3. \tag{6}$$

The ground and equilibrium state bondlengths r_0 and r_e of $^{12}C^{80}Se_2$ and $^{13}C^{80}Se_2$ were determined from the respective rotational constants using the relations (Ref. (*8*))

$$I = 2mr^2 = \frac{16.857629}{B} \text{ amu Å}^2 \tag{7}$$

with $m(^{80}Se) = 79.9165253$ amu.

The vibrational parameters ω_i, x_{ij}, and g_{22} were determined from the ν_0 values according to

$$E_v = \sum_i \omega_i(v_i + 1/2d_i) + \sum_{i\leq j} x_{ij}(v_i + 1/2d_i)(v_j + 1/2d_j) + g_{22}l^2. \tag{8}$$

TABLE IV

Molecular Parameters of $^{12}C^{80}Se_2$ and $^{13}C^{80}Se_2$

$^{12}C^{80}Se_2$						
(cm^{-1})	ν_1^0	369.133 1(12)[a]	ν_2^0	313.090 7(11)	ν_3^0	1301.877 4(5)
(cm^{-1})	ω_1	374.490 3(29)	ω_2	314.378(3)		
(cm^{-1})	x_{11}	-0.174 9(3)	x_{22}	1.286 2(6)	x_{13}	-4.163 26(11)
(cm^{-1})	x_{12}	-2.925 8(11)	g_{22}	-1.005 4(3)	x_{23}	-5.354 96(13)
($10^{-5}cm^{-1}$)	α_1^B	4.069(14)	α_2^B	-7.870(3)	α_3^B	23.708 4(2)
($10^{-5}cm^{-1}$)			q_2	1.074 3(13)		
($10^{-10}cm^{-1}$)	β_1	0.053(5)[b]	β_2	0.246(18)	β_3	0.023 8(6)
($10^{-5}cm^{-1}$)	B_0	3677.325(8)	B_e	3683.344(18)		
($10^{-10}cm^{-1}$)	D_0	14.494(16)	D_e	14.21(4)		
(Å)	r_0	1.693 553 6(19)	r_e	1.692 169(3)		
$^{13}C^{80}Se_2$						
(cm^{-1})	ν_3^0	1254.903 5(5)	x_{13}	-4.016 87(20)	x_{23}	-4.960 21(21)
($10^{-5}cm^{-1}$)	α_1^B	4.04(4)	α_2^B	-7.562(18)	α_3^B	22.795 2(4)
($10^{-5}cm^{-1}$)			q_2	1.125(10)		
($10^{-5}cm^{-1}$)	B_0	3677.448(13)	B_e	3683.30(3)		
(Å)	r_0	1.693 525(3)	r_e	1.692 179(7)		

[a] Figures in parentheses comprise standard deviations of fits and possible calibration errors, see text. [b] Estimated from the (10^01 - 00^00) transition assuming additivity of β_1 and β_3.

Table V summarizes the rovibrational parameters of all vibrational states studied in the present investigation. The vibrational term values G_v account for the propagation of possible calibration errors. Except for the (03^l0) states all vibrational energies were directly derived from measured transitions while those of the latter were calculated from ν_2^0, x_{22}, and g_{22}.

V. PERTURBATION OF THE (30^01) STATE

In the evaluation of the hot band $(30^01\text{–}20^00)$ we noticed that, approaching $J' = 68$ from the lower and higher J values, transitions were increasingly shifted from their expected positions to the higher and lower wavenumbers, respectively. Since independent evidence for the unperturbed nature of the (20^00) state was available we concluded that a level crossing almost exactly between $J' = 67$ and 69, respective

TABLE V

Parameters of Vibrational States of $^{12}C^{80}Se_2$

State	Symmetry	$G_v - G_0$ (cm^{-1})	B_v ($10^{-5} cm^{-1}$)	q_v ($10^{-5} cm^{-1}$)
00^00	Σ_g^+	0.0	3677.325(8)	-
01^10	Π_u	313.090 7(11)	3685.194(11)	1.074 3(13)
10^00	Σ_g^+	369.133 1(12)	3673.256(12)	-
02^20	Δ_g	626.743 1(22)	3693.006(27)	-
02^00	Σ_g^+	630.764 5(22)	3692.37(4)	-
11^10	Π_u	679.224 4(22)	3681.554(28)	1.117(20)
20^00	Σ_g^+	737.916 4(25)	3669.26(5)	-
03^30	Φ_u	940.957(5)	3700.90(6)	-
03^10	Π_u	949.000(5)	3699.62(10)	2.06(9)
12^20	Δ_g	990.181(4)	3689.99(6)	-
12^00	Σ_g^+	993.798(4)	3689.02(8)	-
21^10	Π_u	1045.445(4)	3677.95(3)	1.158(25)
30^00	Σ_g^+	1106.308(5)	3665.24(5)	-
00^01	Σ_u^+	1301.877 4(5)	3653.616(8)	-
01^11	Π_g	1609.613 1(16)	3661.570(11)	1.068 6(20)
10^01	Σ_u^+	1666.847 2(10)	3649.619(11)	-
02^21	Δ_u	1917.918 8(27)	3669.467(27)	0.003 23(26)
02^01	Σ_u^+	1922.019 0(27)	3668.80(4)	-
11^11	Π_g	1971.607 3(21)	3657.954(12)	1.108 4(15)
20^01	Σ_u^+	2031.456 9(22)	3645.549(28)	-
03^31	Φ_g	2226.942(6)	3677.45(6)	-
03^11	Π_g	2234.837(6)	3676.12(10)	2.05(9)
12^21	Δ_u	2277.102(3)	3666.225(27)	-
12^01	Σ_u^+	2280.805(3)	3665.47(8)	-
21^11	Π_g	2333.533(3)	3654.334(28)	1.158(25)
43^10	Π_u	2393.59(5)	3685.8(9)	-
30^01	Σ_u^+	2395.670(4)	3641.50(5)	-

displacement +0.040 and −0.045 cm^{-1}, was present with a perturber whose zero-order energy was smaller, but which had a substantially larger B value than the (30^01) state. Later, this perturbation was also found in the hot band $(30^01–30^00)$.

A quantitative analysis revealed that the data clearly favored a perturbation mechanism with a $[J(J+1)]^{1/2}$-dependent matrix element, as associated with a $\Delta l = \pm 1$ interaction, rather than a Fermi-type or $\Delta l = \pm 2$ mechanism with $[J(J+1)]^0$ and $[J(J+1)]^1$ dependence, respectively. Furthermore, an anharmonic interaction can be ruled out because it would require a Σ_u^+-type perturber for which a v_3 component is compulsory. Such a perturber cannot be constructed with reasonable assumptions concerning anharmonicity. Finally, a v_3 component would make its B value incompatible with the experimental observations.

We propose the (43^10) state as the most reasonable perturber. Its energy $G' - G_0$ calculated employing the data of Table IV according to

$$G' - G_0 = 4\nu_1^0 + 3\nu_2^0 + 12x_{11} + 6x_{22} + 12x_{12} - 2g_{22} \tag{9}$$

is 2388.324(29) cm^{-1} and only 5.2 cm^{-1} smaller than that observed (Table V). Its estimated B value, 3685×10^{-5} cm^{-1}, is in agreement with the experimental value, $3685.8(9) \times 10^{-5}$ cm^{-1}. The 5.2 cm^{-1} deficiency in vibrational energy is obviously due to the importance of higher order anharmonic constants neglected in the calculation of the vibrational energy according to Eq. (9).

The Coriolis-type interaction was accounted for by a matrix element (Ref. (*14*)) given by

$$\begin{aligned}\langle v_1 = 3, v_2^l = 0, v_3 = 1, l = 0, J|\mathbf{H}|v_1 = 4, v_2^l = 3, v_3 = 0, l = -1, J\rangle \\ = W[J(J+1) - l(l \pm 1)]^{1/2}.\end{aligned} \tag{10}$$

The molecular parameters related to the (30^01) state and its perturbation are given in Table VI.

TABLE VI

Analysis of the (30^01) State of $^{12}C^{80}Se_2$ (cm^{-1})

	$(30^01\text{-}20^00)$	$(30^01\text{-}30^00)$
ν_0	1657.753 82(8)[a]	1289.362 21(10)
$B'' \times 10^5$	3669.26(5)	3665.24
$(B''-B') \times 10^5$	27.757 4(28)	23.740 3(12)
$B' \times 10^5$	3641.50	3641.50fix
$D_J'' \times 10^{10}$	14.61(22)	14.724
$(D_J''-D_J') \times 10^{10}$	-0.124(18)	0.0
$D_J' \times 10^{10}$	14.724	14.724fix
$\nu_0-\nu_{(\text{perturber})}$	2.08(4)	2.08fix
$B_{(\text{perturber})} \times 10^5$	3685.8(9)	3685.8fix
$D_{J(\text{perturber})} \times 10^{10}$	14.724fix	14.724fix
$W \times 10^4$	9.67(7)	9.67fix
$\sigma \times 10^5$	26	33

[a] One standard deviation in parentheses.

VI. DISCUSSION

The present study of an isotopically highly enriched CSe_2 sample is the first high-resolution infrared investigation in which the vibration–rotation transitions ν_1, ν_2 and ν_3 have been measured with an accuracy of the order of 1×10^{-3} cm^{-1}, all vibrational states up to 1000 cm^{-1} above the ground state and many higher states experimentally deduced, and the rotational parameters B_v, D_v, and q_v determined. Fewer, but correspondingly accurate data of $^{13}C^{80}Se_2$, $^{12}C^{78}Se^{80}Se$, and $^{12}C^{80}Se^{82}Se$ have been obtained as well, and a large isotopic dependence of ν_3, α_i^B, and x_{ij} is evident from these data. While the B_0 values of $^{12}C^{80}Se_2$ and $^{13}C^{80}Se_2$ differ, the B_e values are, as expected, identical within one standard deviation.

Ground and equilibrium state CSe bondlengths have been determined which are more accurate than the best hitherto available values (*8*) by two orders of magnitude. The correctness of the previous study by Maki and Sams (*8*) is not only confirmed by the consistent B and r values but also by the consistency of their directly measured vibrational energies of the (02^01) and (20^01) states, 1922.0135(10) ± 0.006 and 2031.4504(14) ± 0.006 cm^{-1}, with our values which follow from combination differences, 1922.0190(27) and 2031.4569(22) cm^{-1}, respectively.

Beyond the evaluation of the local $\Delta l = \pm 1$ perturbation pertinent to the (30^01) state, the present study offers an opportunity to search for indications of other resonances, in particular those corresponding to the well-known $10^00/02^00$ resonance between the Σ_g^+ states of CO_2 and CS_2. Sensitive tools among others for this purpose are the rotational constants B_v and q_v. One observation concerns the Δ_g state (02^00) and the transition from it to the (02^01) state. Here, significant evidence for a raised degeneracy of the lower, upper, or both states follows from the effective q values (Table II). Exactly the same observation has been reported for CS_2 by Lindenmayer and Jones (*4*). This effect is not evident from the lower state combination difference analysis of the (02^00) state (Table III) because this is restricted to J values smaller than those associated with the R-branch head.

Concerning the $10^00/02^00$ resonance, CSe_2 differs from its lighter homologs CO_2 and CS_2 because now these two states have an effective energy difference of ~260 cm^{-1} (cf., CO_2 ~100 and CS_2 ~140 cm^{-1}). In light of k_{122} decreasing from CO_2 to CSe_2, interactions between the (10^00) and (02^00) states should be much weaker in the latter. However, the Σ_g^+ states (20^00) and (02^00) (and other corresponding excited states) are quite close, $\Delta\nu \sim 107$ cm^{-1}, and interactions may well become important. The significantly different B values ($\Delta B \sim 7 \times 10^{-6}$ cm^{-1}) of the (02^00) and (02^20) states may be indicative of a fractional mixing of the wavefunctions of the (20^00) and (02^00) states, although the relation $\Delta B/B$ is smaller than in CS_2 and CO_2. A general rovibrational analysis similar to that recently described for OCS (*15*) and CS_2 (*13*) as well as additional experimental data, e.g., such related to x_{33} and ω_3, are also desirable for CSe_2.

ACKNOWLEDGMENTS

We thank K. Lattner for technical assistance. We express our gratitude to the Deutsche Forschungsgemeinschaft for a grant to purchase the FT interferometer and for financial support through SFB 42.

RECEIVED: August 18, 1987

REFERENCES

1. R. Paso, J. Kauppinen, and R. Antilla, *J. Mol. Spectrosc.* **79**, 236–253 (1980).
2. G. Guelachvili, *J. Mol. Spectrosc.* **79**, 72–83 (1980).
3. K. Jolma and J. Kauppinen, *J. Mol. Spectrosc.* **82**, 214–219 (1980).
4. J. Lindenmayer and H. Jones, *J. Mol. Spectrosc.* **110**, 65–73 (1985).
5. B. Rathke, *Liebigs Ann. Chem.* **152**, 181–220 (1869).
6. G. W. King and K. Srikameswaran, *J. Mol. Spectrosc.* **29**, 491–494 (1969).
7. G. W. King and K. Srikameswaran, *J. Mol. Spectrosc.* **31**, 269–291 (1969).
8. A. G. Maki and R. L. Sams, *J. Mol. Spectrosc.* **90**, 215–221 (1981).
9. W. Gombler and H. Willner, *J. Phys. E.* **20**, (1987).
10. G. M. Plummer, G. Winnewisser, M. Winnewisser, J. Hahn, and K. Reinartz, *J. Mol. Spectrosc.* **126**, 255–269 (1987).
11. G. Guelachvili and K. Narahari Rao, "Handbook of Infrared Standards," Academic Press, Orlando, 1986.
12. A. G. Maki and R. L. Sams, *J. Mol. Spectrosc.* **52**, 233–243 (1974).
13. G. Blanquet, E. Baeten, I. Cauuet, J. Walrand, and C. P. Courtoy, *J. Mol. Spectrosc.* **112**, 55–70 (1985).
14. A. G. Maki, W. B. Olson, and R. L. Sams, *J. Mol. Spectrosc.* **36**, 433–447 (1970).
15. A. Fayt, R. Vandenschaute, and J. G. Lahaye, *J. Mol. Spectrosc.* **119**, 233–266 (1986).